Electronic Supplementary Information

Dendritic polyphenylene AIEgens: fluorescent detection of explosives and stimulus-responsive luminescence

Xindong Liu,[a] Yitong Wang,[a] Xiaoqing Liu,[b] Sheng Liu,[a] Yifan Li,[a] Lei Wang[a] and Yi Liu*[a,c]

[a.] *Shenzhen Key Laboratory of Polymer Science and Technology, Guangdong Research Center for Interfacial Engineering of Functional Materials, College of Materials Science and Engineering, Shenzhen University, Shenzhen 518060, China. E-mail: liuyiacee@szu.edu.cn.*

[b.] *Institute of Critical Materials for Integrated Circuits, Shenzhen Polytechnic, Shenzhen, 518055, China.*

[c.] *Centre for AIE Research, Shenzhen University, Shenzhen 518060, China.*

Table of content

1. General materials

Materials: Phenyl ether (Ph_2O), ethanol, Dichloromethane, Petroleum ether. We main p urchased from Energy Chemical (Shanghai, China). All these materials are analytical grade and used as received.

Characterizations and instruments: ^1H, ^{13}C NMR spectra, 2D ^1H-^1H correlation spectroscopy (COSY), nuclear over hauser effect spectroscopy (NOESY) and heteronuclear singular quantum correlation (HSQC) were measured on a Bruker AVANCE III 400MHz, 500MHZ or 600MHZ spectrometer using $CDCl_3$ as solvent and tetramethylsilane (TMS, δ = 0) as internal standard. Time-of-flight mass spectrometry (MALDI-TOF/TOF) through Guan Technology Service (Guangzhou) Co., Ltd test. Absorption spectra were taken on a Thermo-fisher Evolution 220 spectrometer. Emission spectra were taken on a Thermo Lumina Fluorescent spectrometer. Powder XRD patterns were recorded on a Rigaku Smart Lab X-ray Diffractometer. Gel permeation chromatography(GPC) were taken on a Agilent 1260 Infinity II separate. The electrochemical workstation is complete with cyclic voltammetry using a Chenhua 760e. The absolute fluorescence quantum yield (QY) was measured using C11347 instrument via integrating sphere. Elementary analysis results were collected on elementar vario EL cube.

2. Synthesis detailes

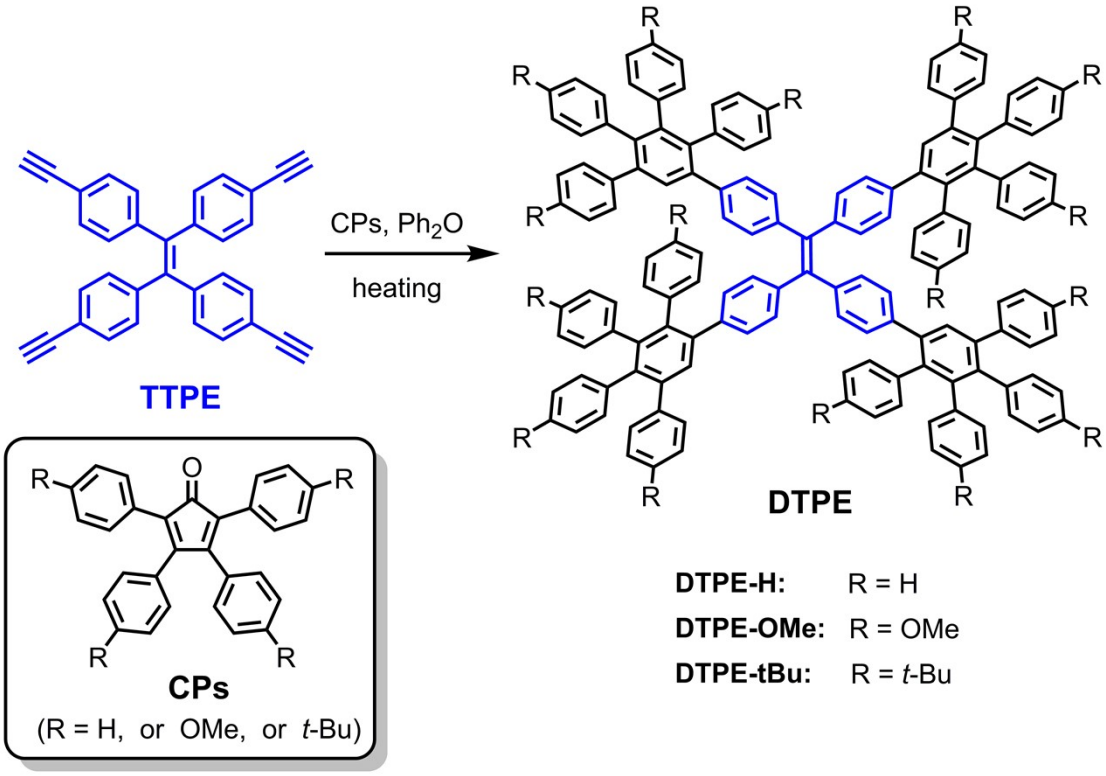

Scheme S1. Synthetic routes toward the dendritic AIEgens **DTPEs**.

The corresponding precursor **TTPE** (1,1′,1″,1‴-(1,2-Ethenediylidene)tetrakis[4-ethynylbenzene]) was synthesized according to the previously literature.[1] The another three precursors (**CPs**) 2,3,4,5-Tetraphenyl-2,4-cyclopentadien-1-one, ,3,4,5-Tetrakis[4-(1,1-dimethylethyl)phenyl]-2,4-cyclopenta-dien-1-one, and 2,3,4,5-tetrakis(4-methoxyphenyl)cyclopenta-2,4-dien-1-one were prepared according to the previously literature.[2]

DTPE-H

To a flask containing compound **TTPE** (1.0 eq, 0.10 g, 0.23 mmol), and 2,3,4,5-Tetraphenyl-2,4-cyclopentadien-1-one (6.0 eq, 0.54 g, 1.40 mmol) was added Phenyl ether (10 ml). The resulting solution was stirred for half a day at 220℃. The resulting solution was slowly dripped into the EtOH (50 mL) to precipitation, and the crude product was further purified by silica-gel chromatography using CH_2Cl_2/n-Hexane mixture (1:1, v/v) as eluent. The titled compound **DTPE-H** was obtained as a gray solid (0.32 g, 73.8% yield). HRMS (MALDI-TOF, DCTB as matrix) m/z: [M]+ calcd. for $C_{146}H_{100}$: 1854.4060. Found: 1853.710. ^{1}H NMR (400 MHz,

Chloroform-*d*) δ 7.54 (s, 1H), 7.15 (p, *J* = 2.1 Hz, 4H), 6.92 (dd, *J* = 3.0, 1.6 Hz, 2H), 6.88 – 6.84 (m, 8H), 6.84 – 6.73 (m, 7H), 6.66 (d, *J* = 8.3 Hz, 2H). ^{13}C NMR (151 MHz, Chloroform-*d*) δ 141.53 (d, *J* = 13.2 Hz), 140.67, 139.94 (d, *J* = 17.1 Hz), 139.17 (d, *J* = 10.1 Hz), 132.96 – 131.35 (m), 130.80 , 129.96 , 129.10 , 127.56 , 126.82 (d, *J* = 16.8 Hz), 126.60 , 125.56 (d, *J* = 4.8 Hz). Elemental analysis: calcd (%): C, 94.56, H, 5.44; found (%): C 94.36, H 5.57.

DTPE-*t*Bu

To a flask containing compound **TTPE** (1.0 eq, 55 mg, 0.125mmol), and 2,3,4,5-Tetrakis[4-(1,1-dimethylethyl)phenyl]-2,4-cyclopentadien-1-one (6.0 eq, 460 mg, 0.75 mmol) was added Phenyl ether (10 ml). The resulting solution was stirred for half a day at 220℃. The resulting solution was slowly dripped into the EtOH (50 mL) to precipitation, and the crude product was further purified by silica-gel chromatography using CH_2Cl_2/n-Hexane mixture (1:1, v/v) as eluent. The titled compound **DTPE-t-Bu** was obtained as a yellow solid (0.2 g, 58.1% yield). HRMS (MALDI-TOF, DCTB as matrix) m/z: [M]+ calcd. for $C_{210}H_{228}$: 2752.1340. Found: 2751.760. ^{1}H NMR (400 MHz, Chloroform-*d*) δ 7.52 – 7.49 (m, 4H), 7.16 – 7.12 (m, 8H), 7.10 – 7.05 (m, 8H), 6.91 – 6.78 (m, 20H), 6.74 – 6.69 (m, 4H), 6.67 – 6.59 (m, 16H), 1.17 – 1.07 (m, 48H). ^{13}C NMR (151 MHz, Chloroform-*d*) δ 148.61 , 147.96 , 147.49 , 141.91 , 141.41 , 140.48 , 140.25 , 139.29 , 139.24 , 139.01 , 137.63 , 137.31 , 137.08 , 131.16 , 131.04 , 130.62 , 130.39 , 129.61 , 129.05 , 124.19 , 123.37 , 123.25 , 123.00 , 34.31 , 34.13 , 34.08 , 34.05 , 31.31 , 31.23 , 31.21.

DTPE-OMe

To a flask containing compound **TTPE** (1.0 eq, 0.20 g, 0.46 mmol), and 2,3,4,5-tetrakis(4-methoxyphenyl)cyclopenta-2,4-dien-1-one (6.0 eq, 1.40 g, 2.77 mmol) was added Phenyl ether (10 ml). The resulting solution was stirred for half a day at 220℃. The resulting solution was slowly dripped into the EtOH (50 mL) to precipitation, and the crude product was further purified by silica-gel chromatography using CH_2Cl_2/n-Hexane mixture (1:1, v/v) as eluent. The titled compound **DTPE-OMe** was obtained as a yellow brown solid (0.41 g, 29.6% yield). HRMS (MALDI-TOF, DCTB as matrix) m/z: [M]+ calcd. for $C_{162}H_{132}O_{16}$: 2334.8220. Found: 2333.736. ^{1}H NMR (500 MHz, Chloroform-*d*) δ 7.46 (s, 4H), 7.10 – 7.01 (m,8H), 6.86 – 6.78 (m, 8H), 6.74 – 6.67 (m, 24H), 6.66 – 6.59 (m,16H), 6.53 – 6.48 (m, 24H), 6.46 – 6.36 (m, 48H), 3.75 (s, 12H), 3.68 (s,

12H), 3.64 (s, 12H), 3.50 (s, 12H). ^{13}C NMR (151 MHz, Chloroform-*d*) δ 157.89 , 157.20 , 156.93 , 141.51 , 140.81 , 140.15 , 138.94 , 138.83 , 134.46 , 133.09 , 132.74 , 132.71 , 132.53 , 132.49 , 132.40 , 131.01 , 130.82 , 129.00 , 113.05 , 112.53 , 112.24 , 112.17 , 55.14 , 54.97 , 54.93 , 54.69 . Elemental analysis: calcd (%): C, 83.34, H, 5.70; found (%): C 83.57, H 6.07.

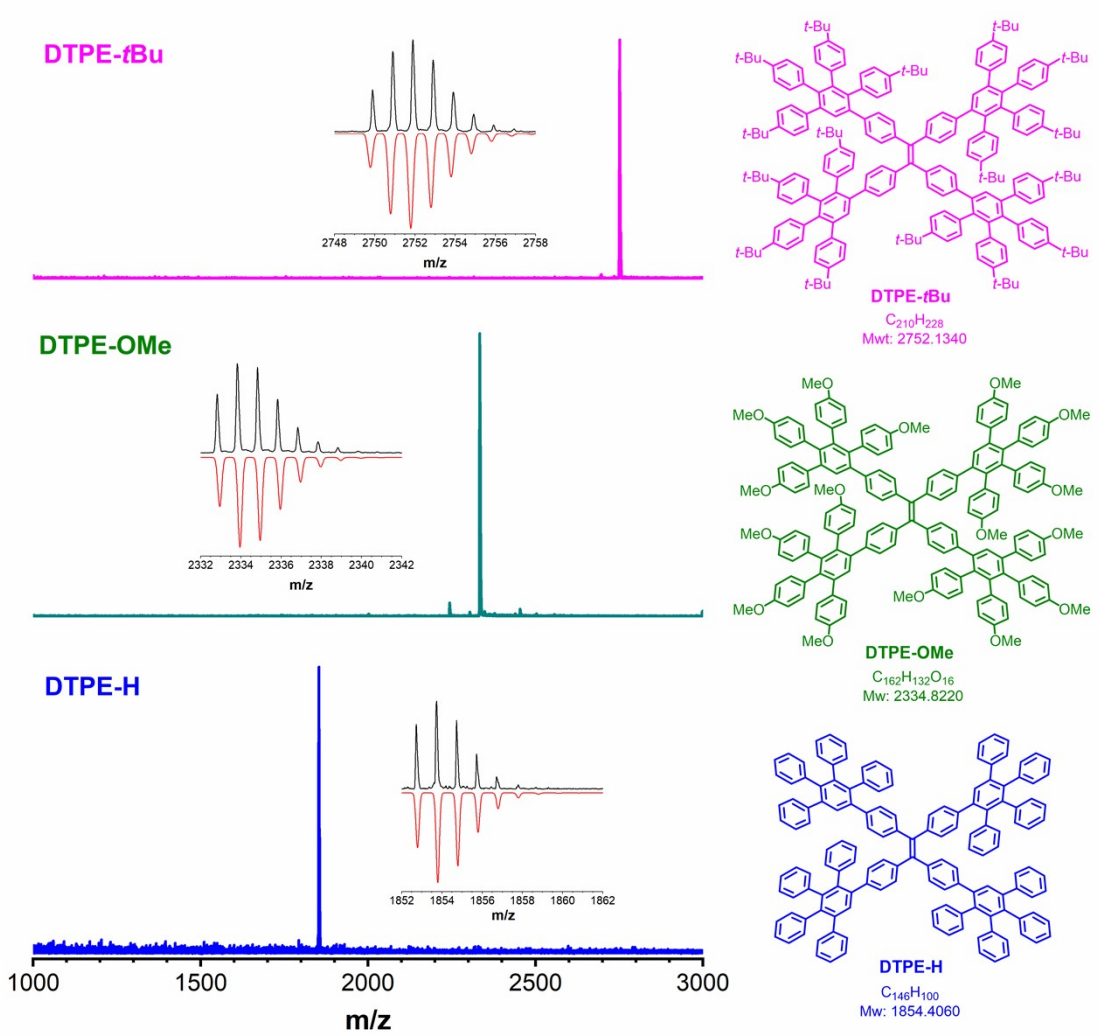

Figure S1. MALDI-TOF mass spectrometry of dendritic AIEgens **DTPEs**. Inset: the experimental and simulated isotropy distributions.

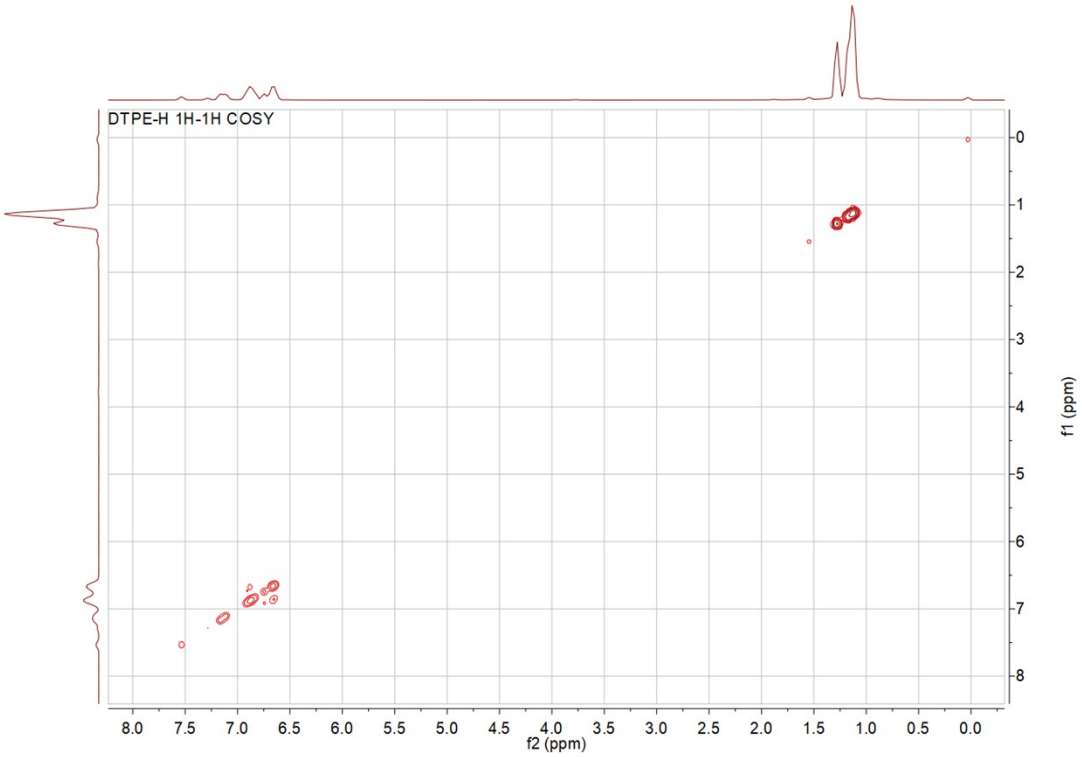

Figure S2. Partial 2D ^{1}H-^{1}H COSY NMR spectrum of **DTPE-*t*Bu** in $CDCl_3$.

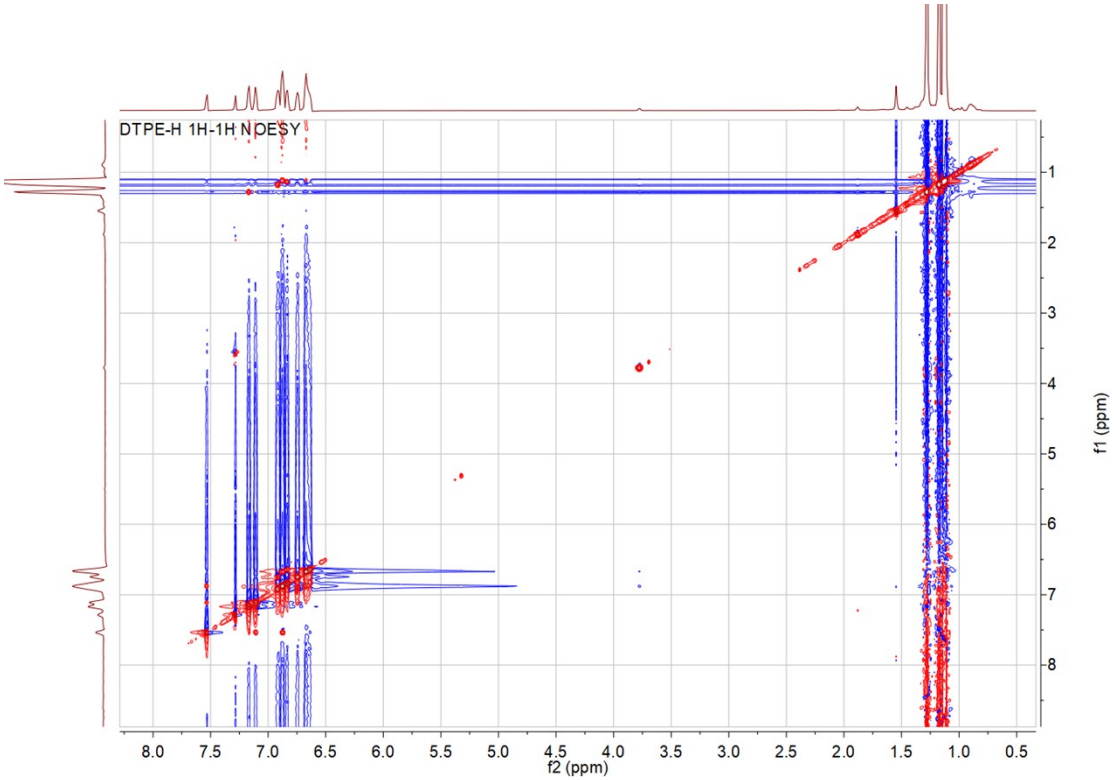

Figure S3. Partial 2D ^{1}H-^{1}H NOESY NMR spectrum of **DTPE-*t*Bu** in $CDCl_3$.

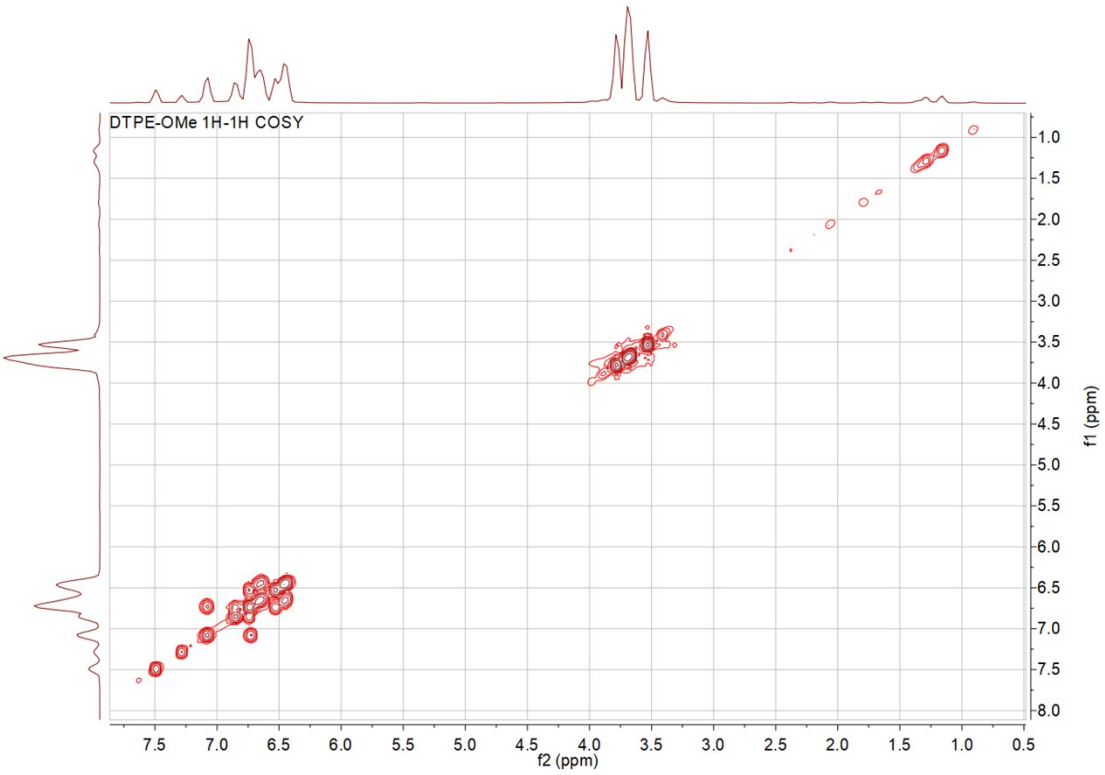

Figure S4. Partial 2D ^{1}H-^{1}H COSY NMR spectrum of **DTPE-OMe** in $CDCl_3$.

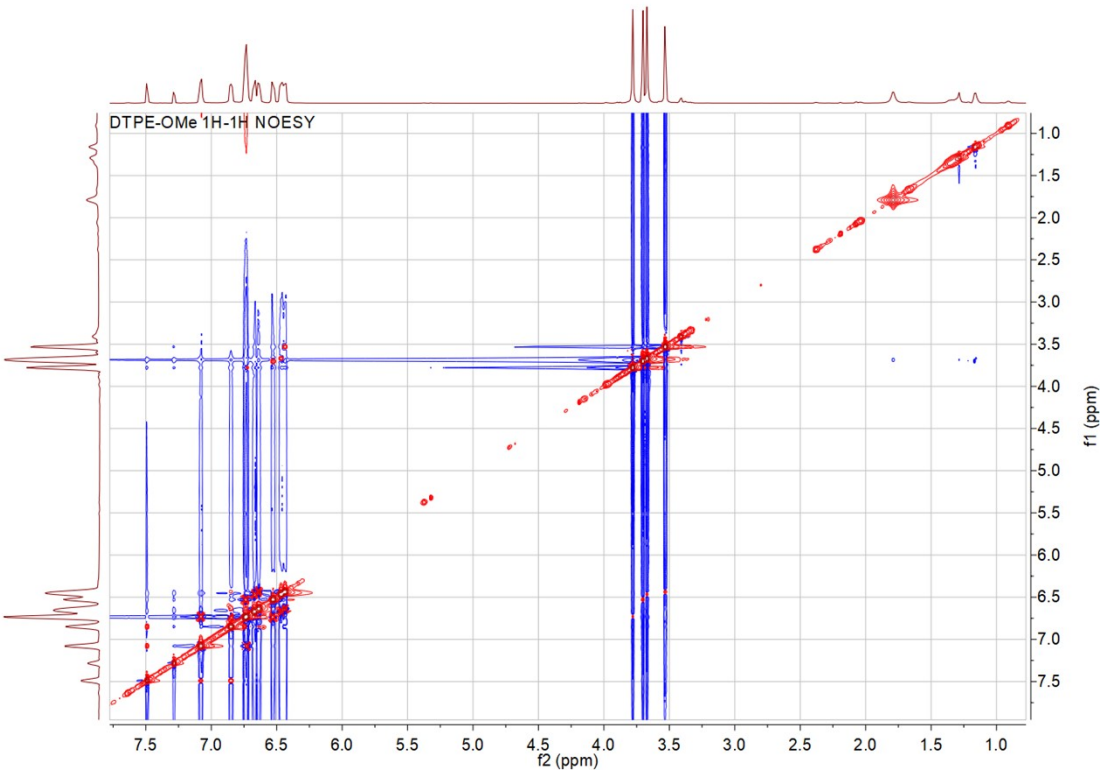

Figure S5. Partial 2D ^{1}H-^{1}H NOESY NMR spectrum of **DTPE-OMe** in $CDCl_3$.

3. Figures and charts

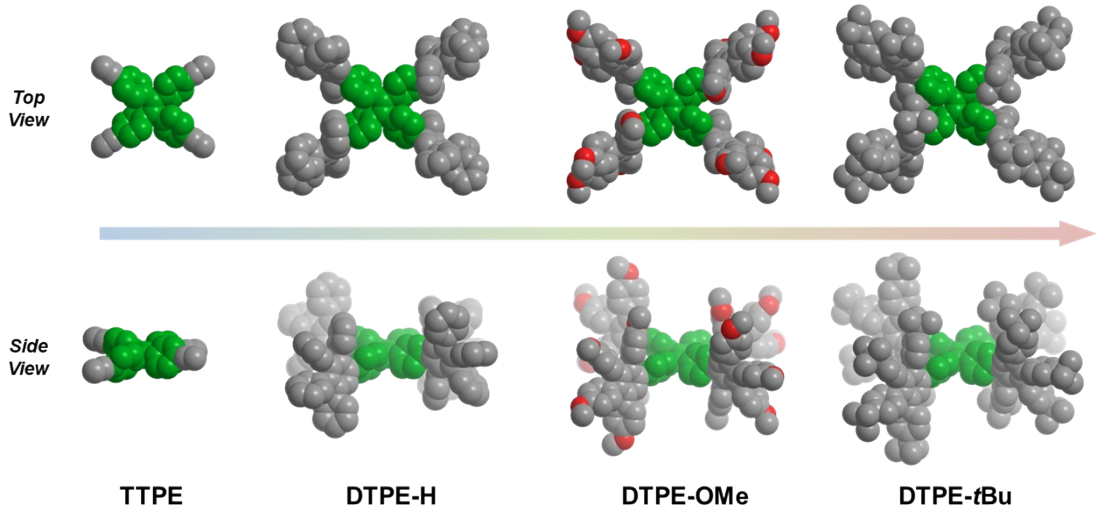

Figure S6 Optimized geometry for **TTPE** and dendritic AIEgens **DTPEs** respectively, based on B3LYP/6-31G level via DFT calculation.

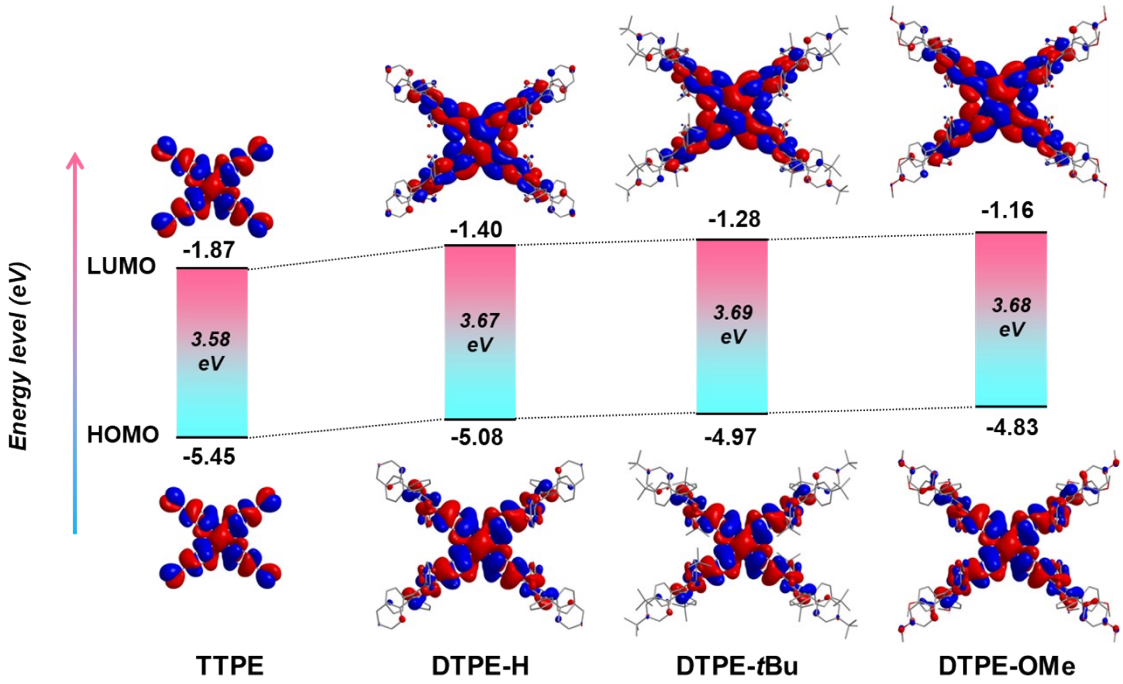

Figure S7. Molecular energy level of for **TTPE** and dendritic AIEgens **DTPEs** respectively, based on B3LYP/6-31G level via DFT calculation.

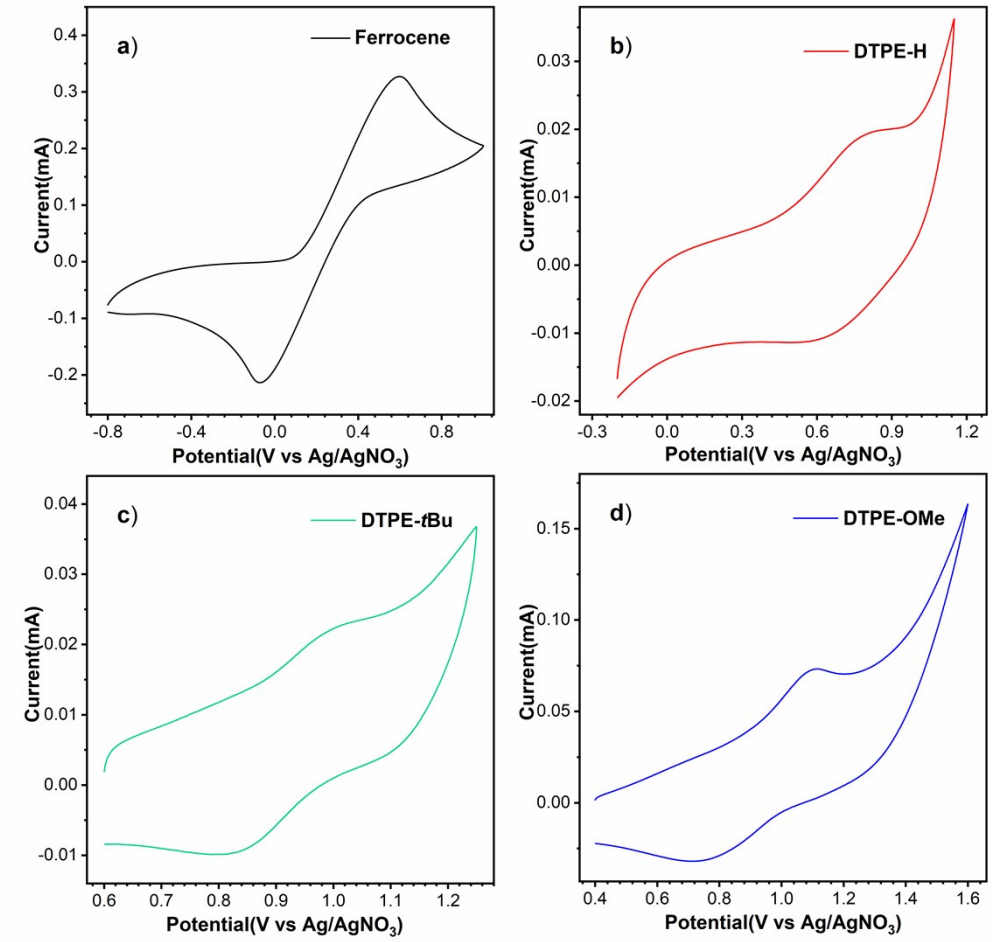

Figure S8. Cyclic voltametry spectra of ferrocene and dendritic AIEgens **DTPEs** in DCM measured with [n-Bu4N][PF6] (0.1 M) as a supporting electrolyte.

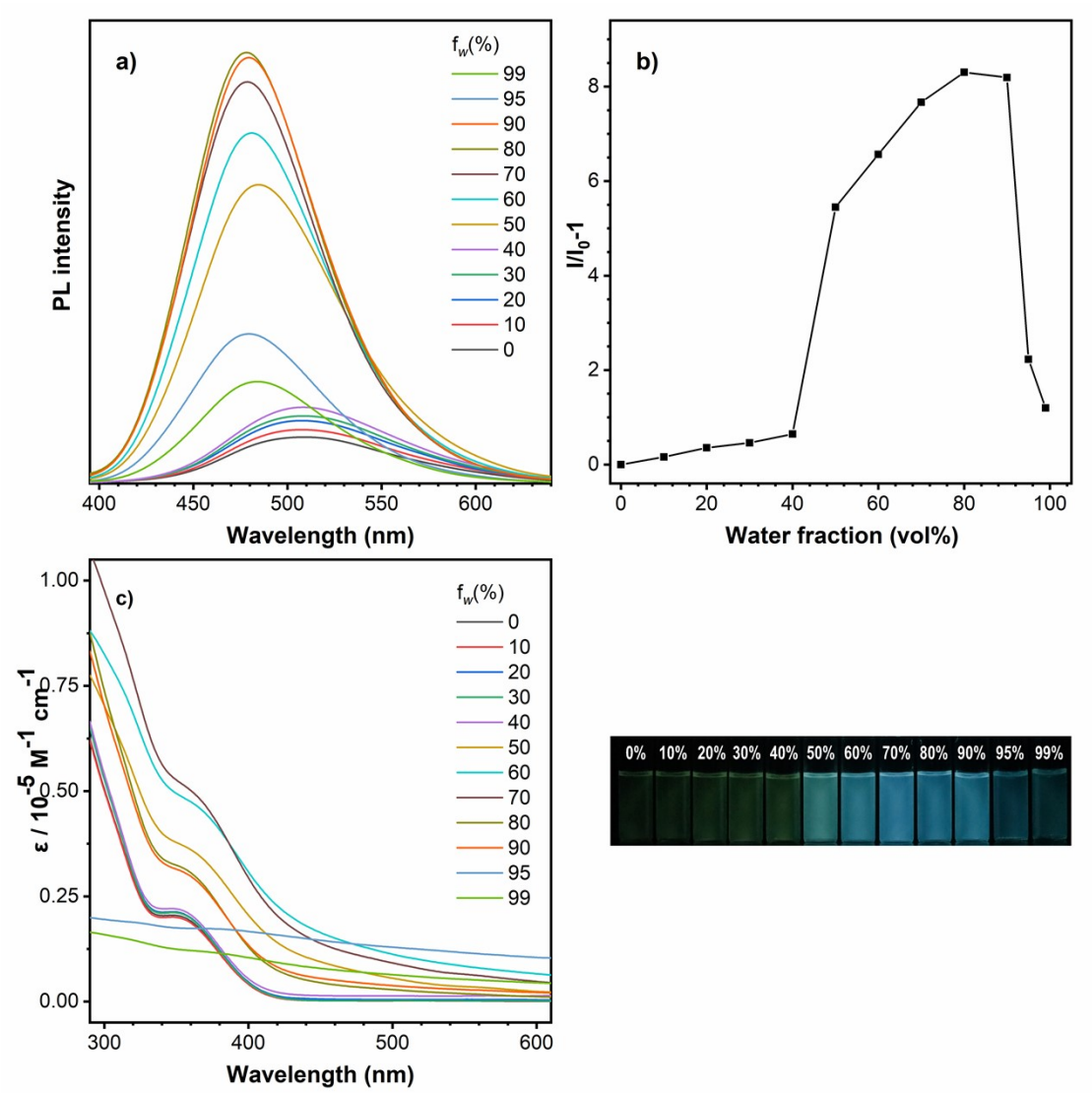

Figure S9. (a) Photoluminescence spectra of dendritic AIEgen **DTPE-H** in THF and THF/water mixtures with different water fraction (f_w). (b) Plots of the maximum emission intensities of **DTPE-H** in THF and THF/water mixtures versus f_w. (c) UV-Vis absorption spectra of dendritic AIEgen **DTPE-H** in THF and THF/water mixtures with different water fraction (f_w). Inset: Images of **DTPE-H** under UV lamp in THF and THF/water mixture with different f_w. Concentration = 10 μM.

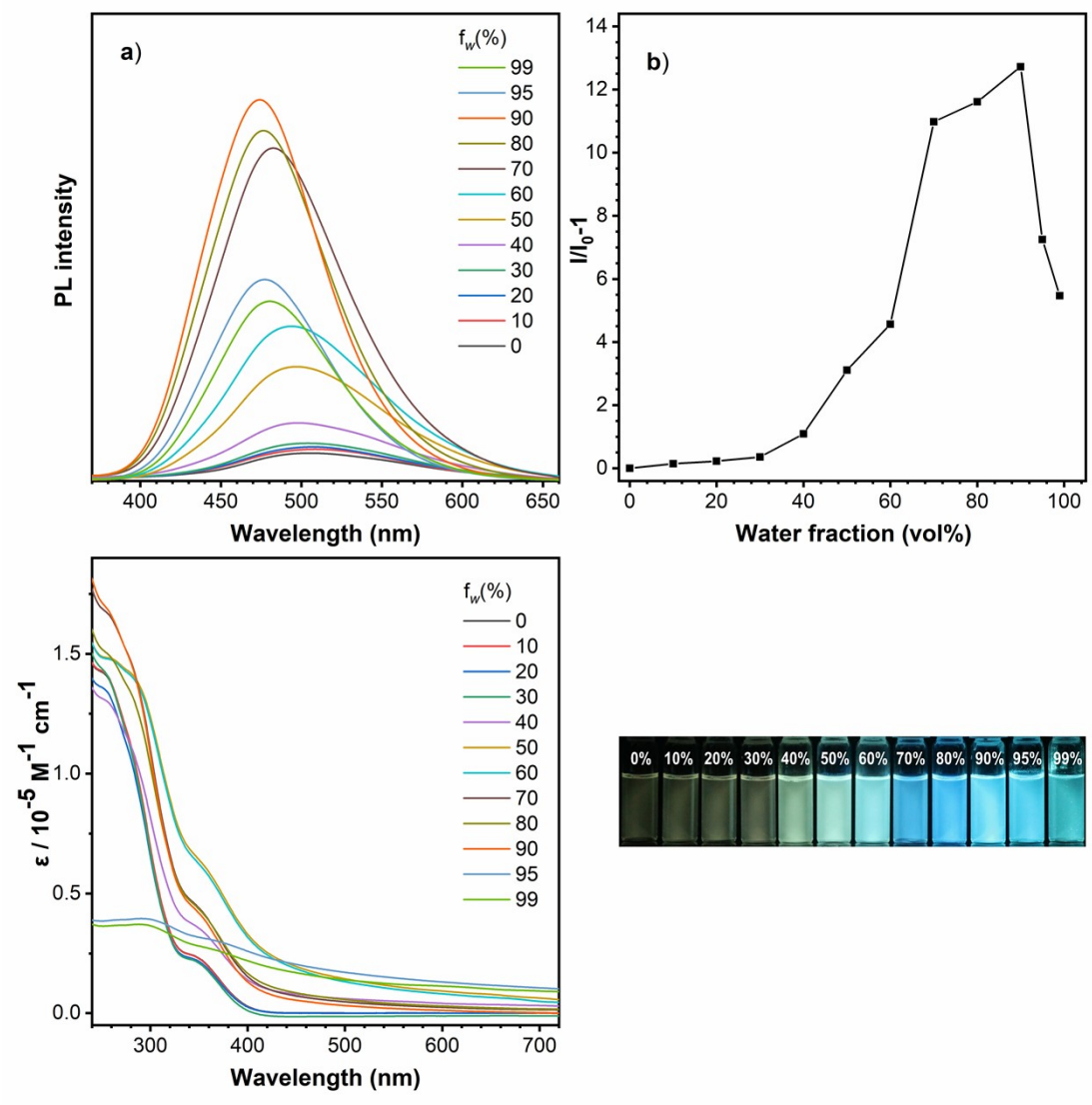

Figure S10. (a) Photoluminescence spectra of dendritic AIEgen **DTPE-*t*Bu** in THF and THF/water mixtures with different water fraction (f_w). (b) Plots of the maximum emission intensities of **DTPE-*t*Bu** in THF and THF/water mixtures versus f_w. (c) UV-Vis absorption spectra of dendritic AIEgen **DTPE-*t*Bu** in THF and THF/water mixtures with different water fraction (f_w). Inset: Images of **DTPE-*t*Bu** under UV lamp in THF and THF/water mixture with different f_w. Concentration = 10 μM.

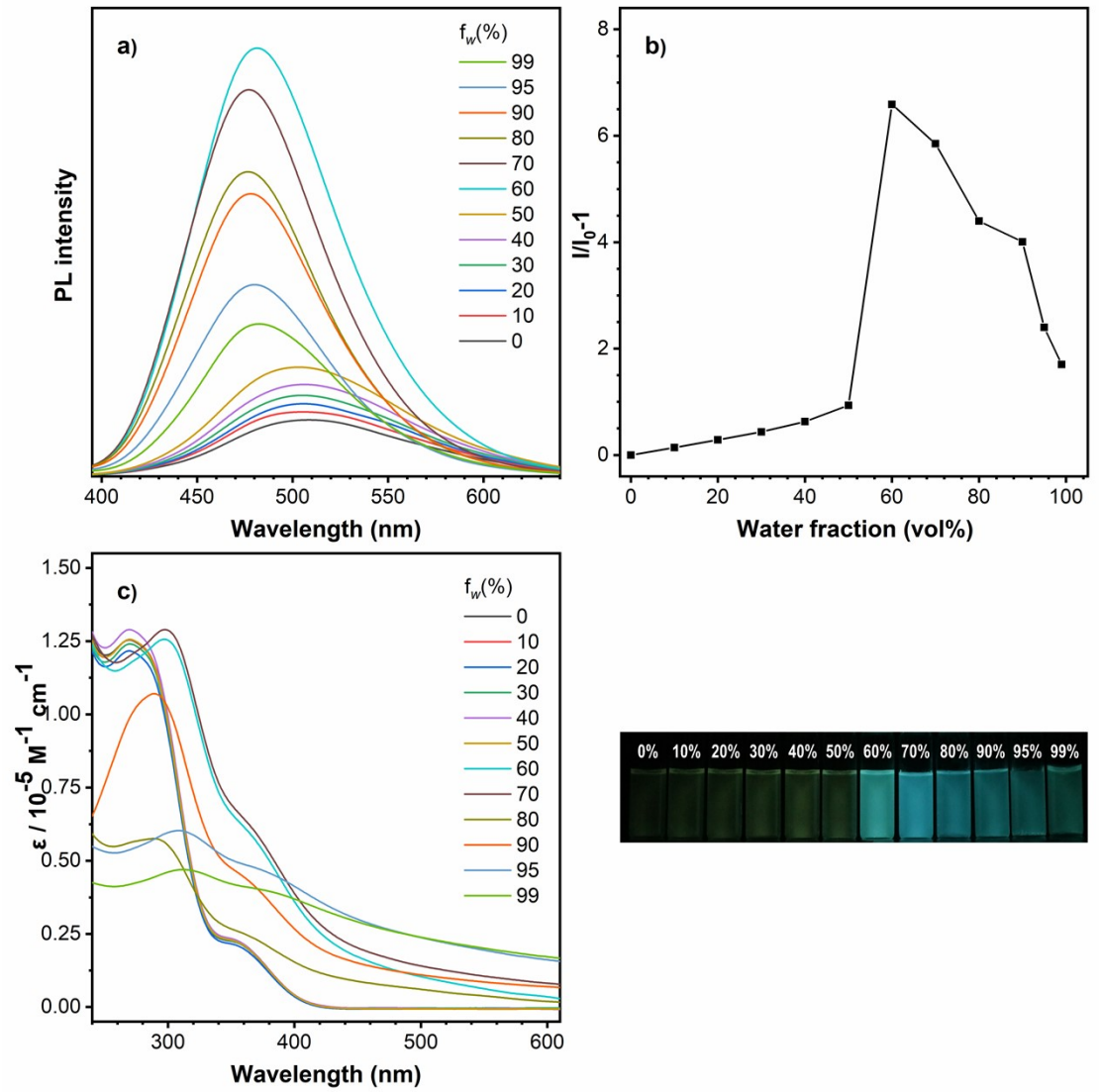

Figure S11. (a) Photoluminescence spectra of dendritic AIEgen **DTPE-OMe** in THF and THF/water mixtures with different water fraction (f_w). (b) Plots of the maximum emission intensities of **DTPE-OMe** in THF and THF/water mixtures versus f_w. (c) UV-Vis absorption spectra of dendritic AIEgen **DTPE-OMe** in THF and THF/water mixtures with different water fraction (f_w). Inset: Images of **DTPE-OMe** under UV lamp in THF and THF/water mixture with different f_w. Concentration = 10 μM.

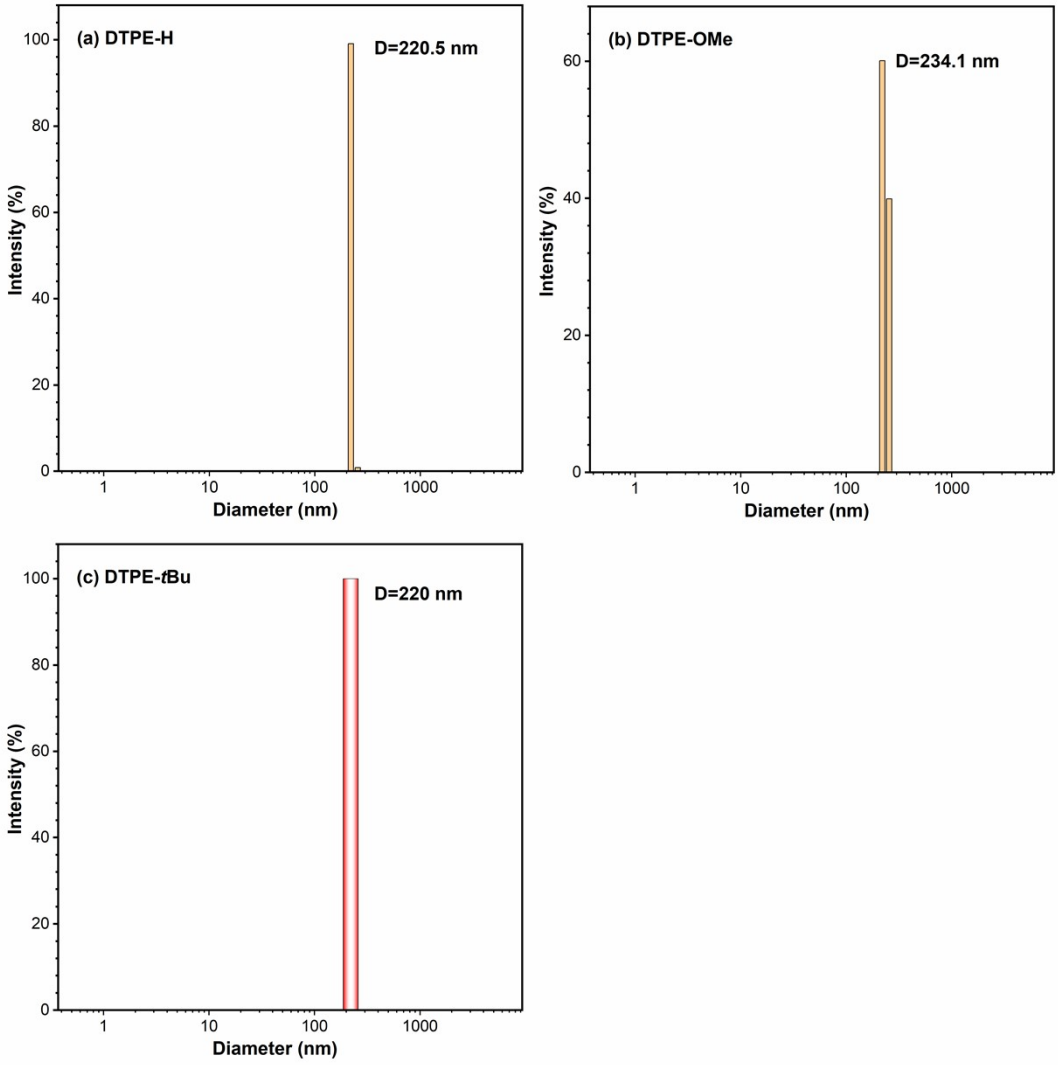

Figure S12. Dynamic light scattering of dendritic AIEgen **DTPEs** in THF/Water mixture with water fraction f_w = 90%.

Table S1. Photo-physical properties of dendritic AIEgens **DTPEs**

	λ_{ab} (nm)	λ_{em}(nm)[b]			E_g [eV] [d]	HOMO [eV]		LUMO [eV]	
		Soln [Φ_F,%][c]	Aggr [Φ_F,%][c]	Powder [Φ_F,%][c]		Exp.[e]	Calc.[f]	Exp.[e]	Calc.[f]
DTPE-H	392	508.6 (12.21%)	479.5 (32.48%)	435 (42.96%)	3.17	-5.02	-5.08	-1.85	-1.40
DTPE-*t*Bu	384	505.2 (14.68%)	475 (36.29%)	486 (44.87%)	3.24	-5.42	-4.97	-2.18	-1.28
DTPE-OMe	388	508.2 (12.58%)	478.1 (27.96%)	491.5 (47.31%)	3.20	-5.46	-4.83	-2.26	-1.16

[a] λ_{ab} = absorption maximum in pure THF.

[b] λ_{em} = emission maximum in pure THF solution (soln), THF/water mixture (1:9 by volume) (aggr).

[c] Fluorescence quantum yield (Φ_F,%) of THF solution and solid powders given in the parentheses.

[d] E_g = energy band gap calculated from the onset of the absorption spectrum.

[e] HOMO = highest occupied molecular orbitals calculated from the onset oxidation potential, LUMO = lowest unoccupied molecular orbitals estimated by the equation: LUMO=HOMO + E_g.

[f] calculated based on B3LYP/6-31G level via DFT calculation

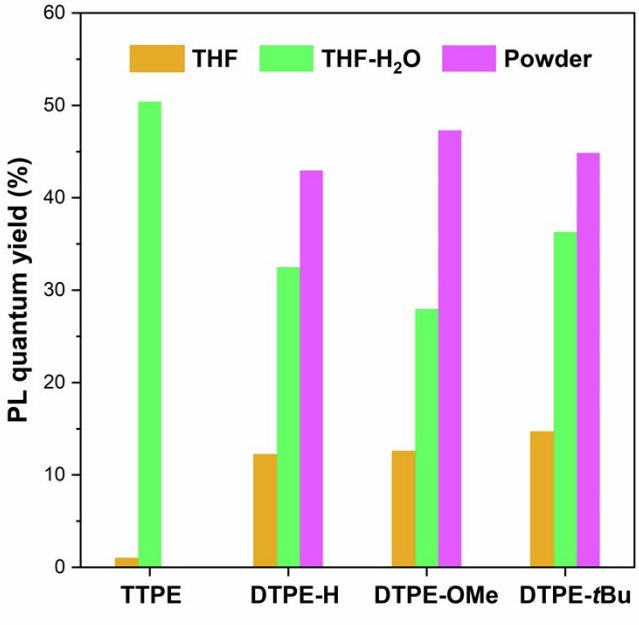

Figure S13. Emission quantum yield of **TTPE** and **DTPEs** in THF, THF-H_2O mixture (f_w = 90%) and solid state.

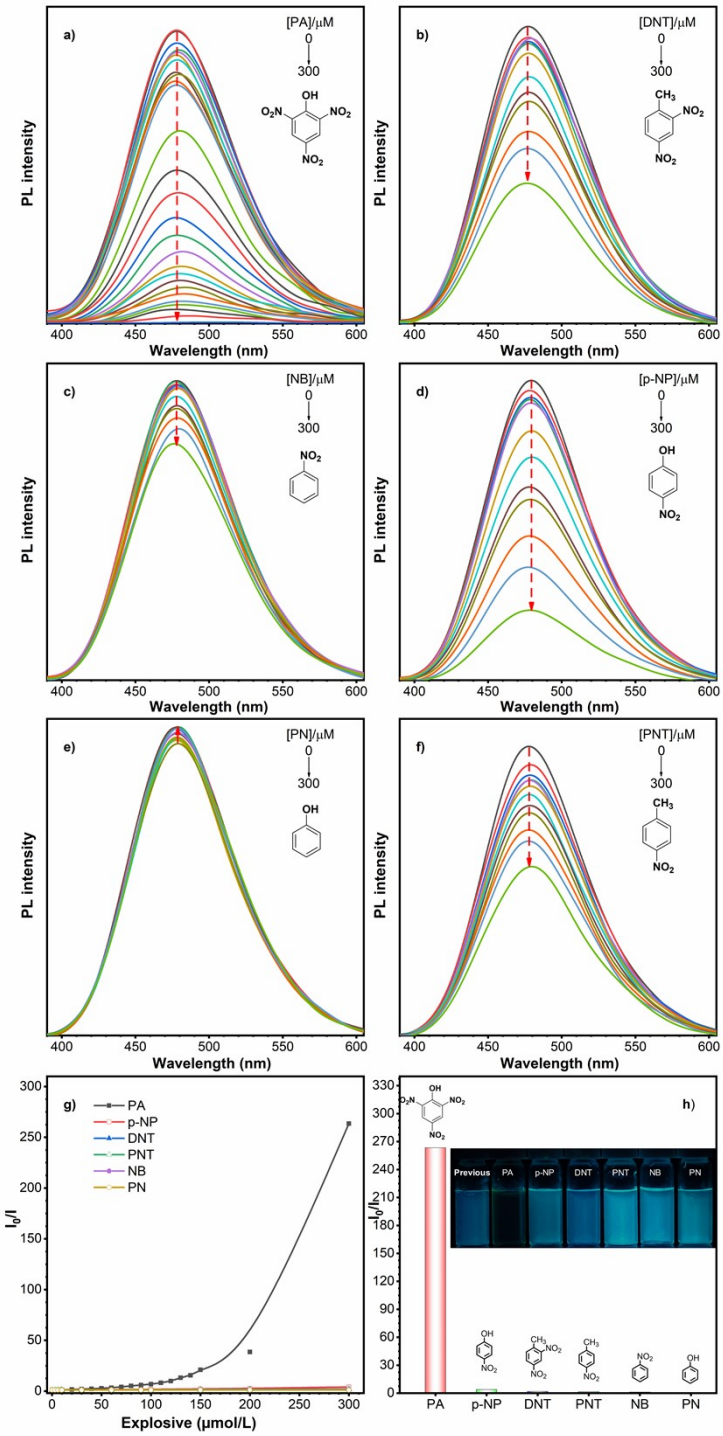

Figure S14. PL spectra of **DTPE-H** in absence and presence of PA (a), *p*-NP (b), DNT (c), *p*-NT (d), NB (e), Ph (f) in THF-H_2O mixture with f_w = 90%. (g) Dependency of fluorescence intensity (I) of **DTPE-H** with nitro-compounds concentration. (h) PL response of **DTPE-H** with different nitro-compounds (300 μM) [**DTPE-H**] = 1 μM. I_0 is the maximal PL intensity in absence of nitro-compounds. Inset: Images of **DTPE-H** under UV lamp in THF/water mixture (f_w = 90%) with 90 μM nitor-compounds.

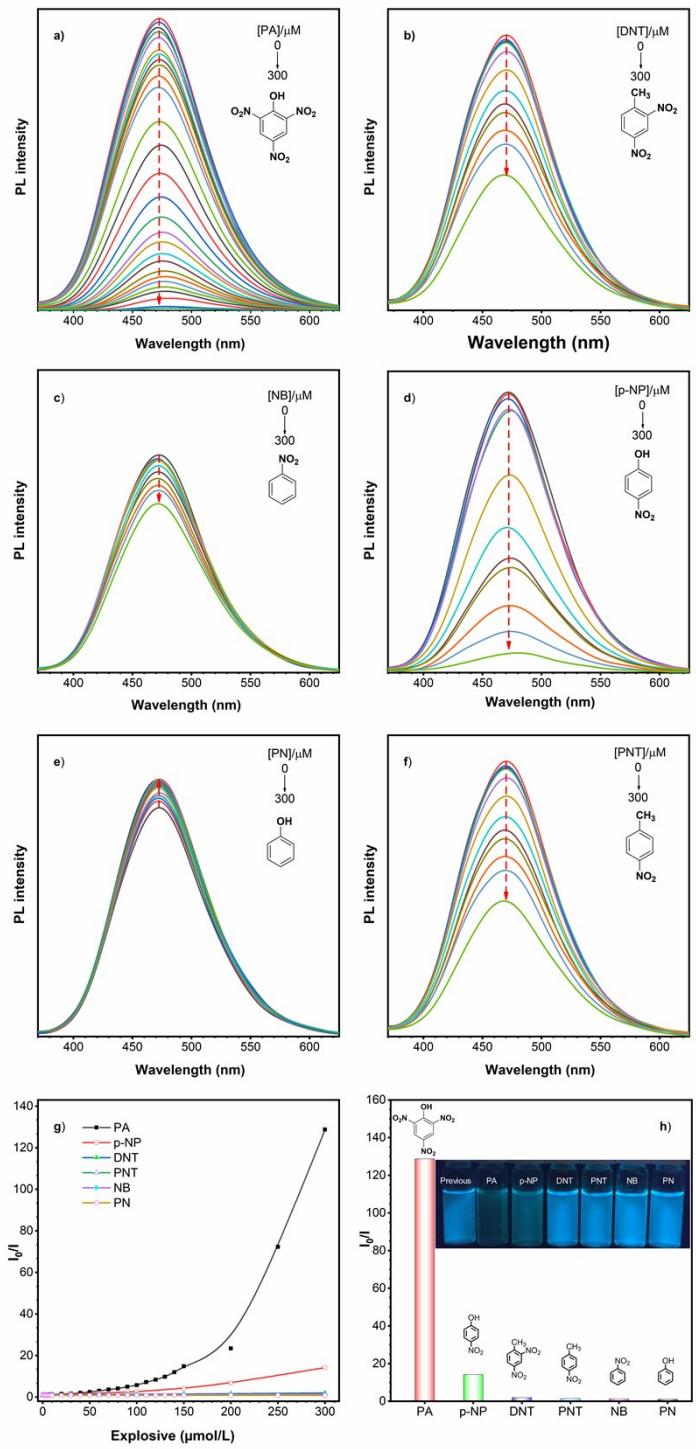

Figure S15. PL spectra of **DTPE-*t*Bu** in absence and presence of PA (a), *p*-NP (b), DNT (c), *p*-NT (d), NB (e), Ph (f) in THF-H_2O mixture with f_w = 90%. (g) Dependency of fluorescence intensity (I) of **DTPE-*t*Bu** with nitro-compounds concentration. (h) PL response of **DTPE-*t*Bu** with different nitro-compounds (300 μM) [**DTPE-*t*Bu**] = 1 μM. I_0 is the maximal PL intensity in absence of nitro-compounds. Inset: Images of **DTPE-*t*Bu** under UV lamp in THF/water mixture (f_w = 90%) with 90 μM nitor-compounds.

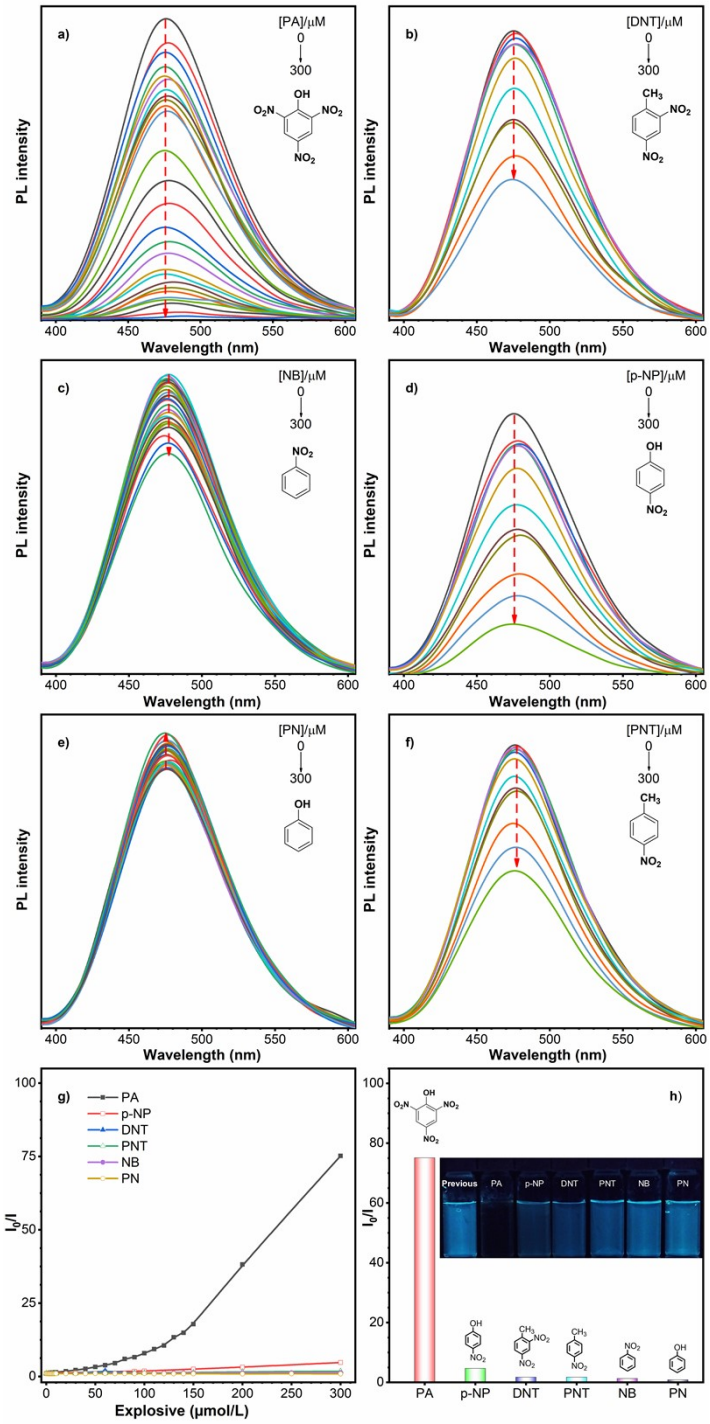

Figure S16. PL spectra of **DTPE-OMe** in absence and presence of PA (a), *p*-NP (b), DNT (c), *p*-NT (d), NB (e), Ph (f) in THF-H_2O mixture with f_w = 90%. (g) Dependency of fluorescence intensity (I) of **DTPE-OME** with nitro-compounds concentration. (h) PL response of **DTPE-OMe** with different nitro-compounds (300 μM) [**DTPE-OMe**] = 1 μM. I_0 is the maximal PL intensity in absence of nitro-compounds. Inset: Images of **DTPE-OMe** under UV lamp in THF/water mixture (f_w = 90%) with 90 μM nitor-compounds.

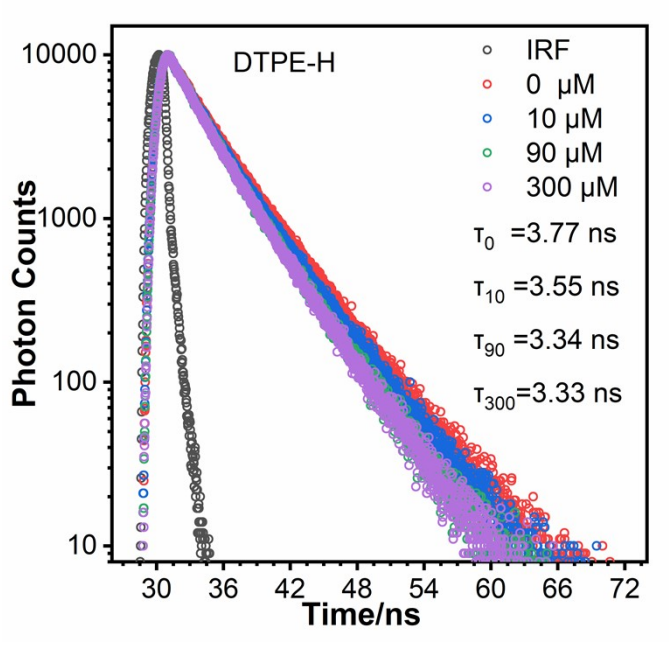

Figure 17. Luminescence lifetime decay of dendritic AIEgen **DTPE-H** suspensions in absence and presence of PA.

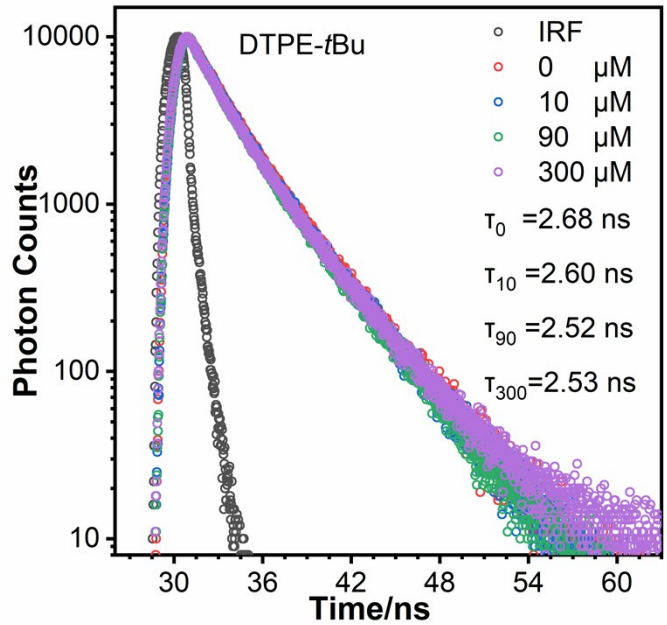

Figure 18. Luminescence lifetime decay of dendritic AIEgen **DTPE-*t*Bu** suspensions in absence and presence of PAs.

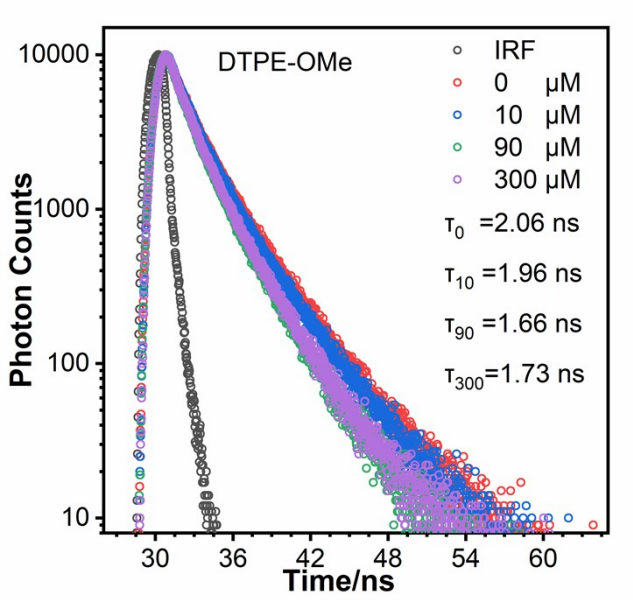

Figure 19. Luminescence lifetime decay of dendritic AIEgen **DTPE-OMe** suspensions in absence and presence of PA.

Table 2. Comparative study of the present system with previously reported fluorescent sensors for PAs

Structure of probe	Solvent	λ_{em}[nm]	K_{SV}/M^{-1}	Ref.
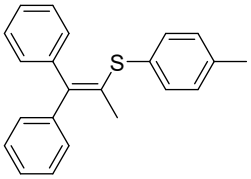	THF/H_2O (1/19)	456	2.99×10^3	[4]
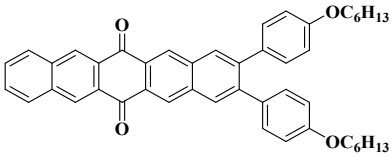	THF/H_2O (1:9)	555	8.44×10^3	[5]
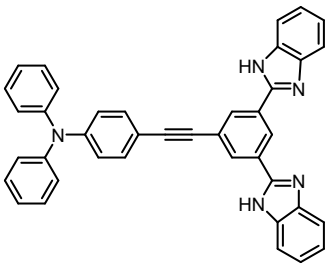	THF/H_2O (1:1)	427	7.43×10^3	[6]
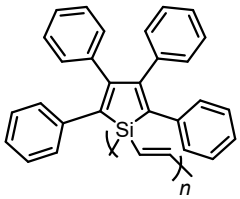	Toluene	493	16.4×10^3	[7]
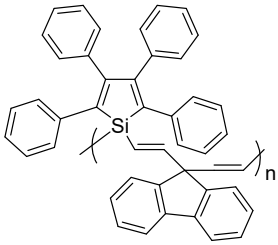	Toluene	492	15.6×10^3	[8]
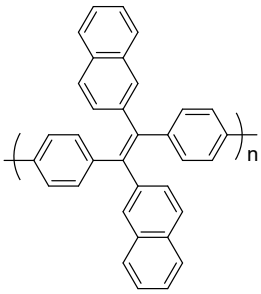	THF/H_2O (1:9)	520	4.204×10^3	[9]

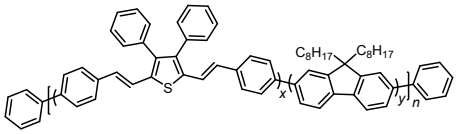	THF/H_2O (1/19)	500	4.456× 10^3	[10]
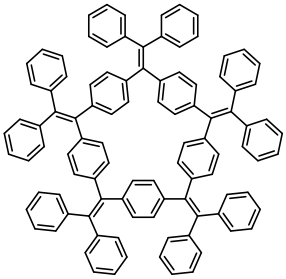	THF/H_2O (1/4)	495	1.79× 10^3	[11]
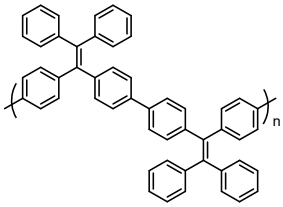	THF/H_2O (1:9)	480	12.2× 10^3	[12]
DTPE-H	**THF/H_2O (1:9)**	**509**	**26.1× 10^3**	**This work**
DTPE-OMe	**THF/H_2O (1:9)**	**508**	**37.4× 10^3**	**This work**
DTPE-*t*Bu	**THF/H_2O (1:9)**	**505**	**27.7× 10^3**	**This work**

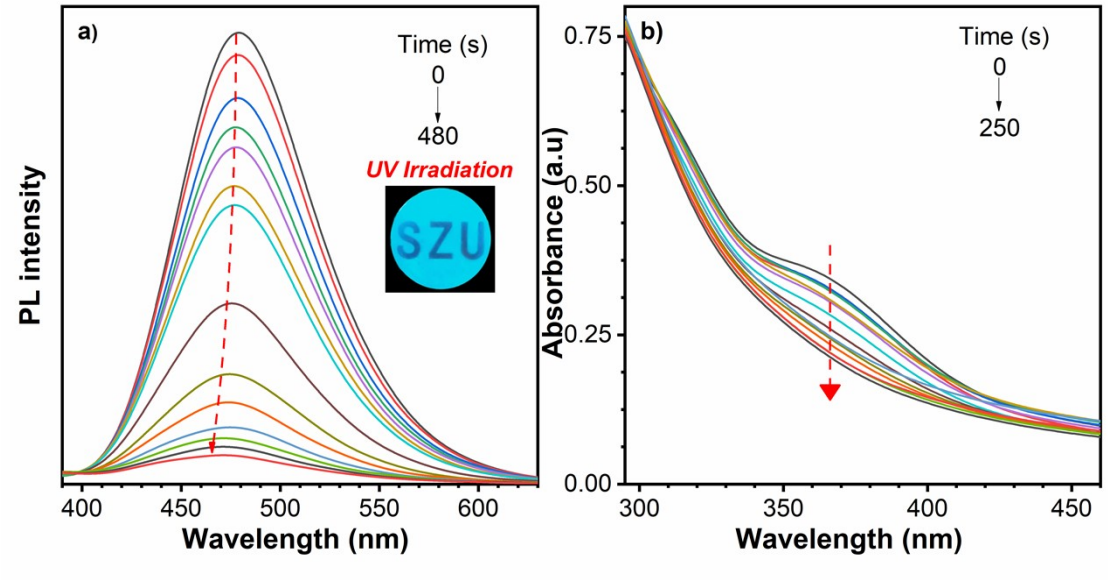

Figure S20. PL spectra (a) and UV-Vis absorption spectra of **DTPE-H** after 365 nm UV light irradaition in THF-H_2O mixture with f_w = 90%. Concentration: 10 uM.

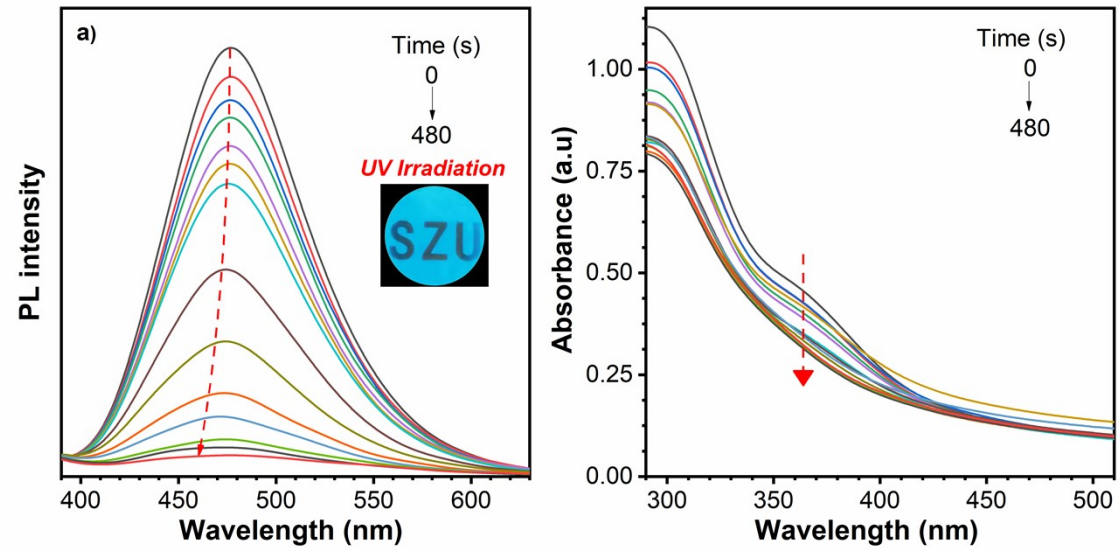

Figure S21. PL spectra (a) and UV-Vis absorption spectra of **DTPE-OMe** after 365 nm UV light irradaition in THF-H_2O mixture with f_w = 90%. Concentration: 10 uM.

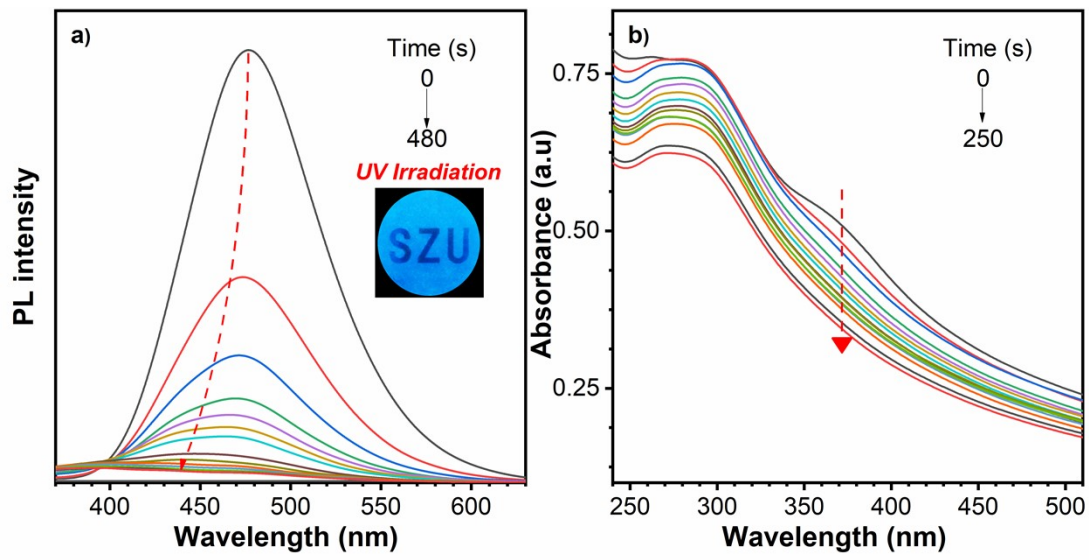

Figure S22. PL spectra (a) and UV-Vis absorption spectra of **DTPE-*t*Bu** after 365 nm UV light irradaition in THF-H_2O mixture with f_w = 90%. Concentration: 10 uM.

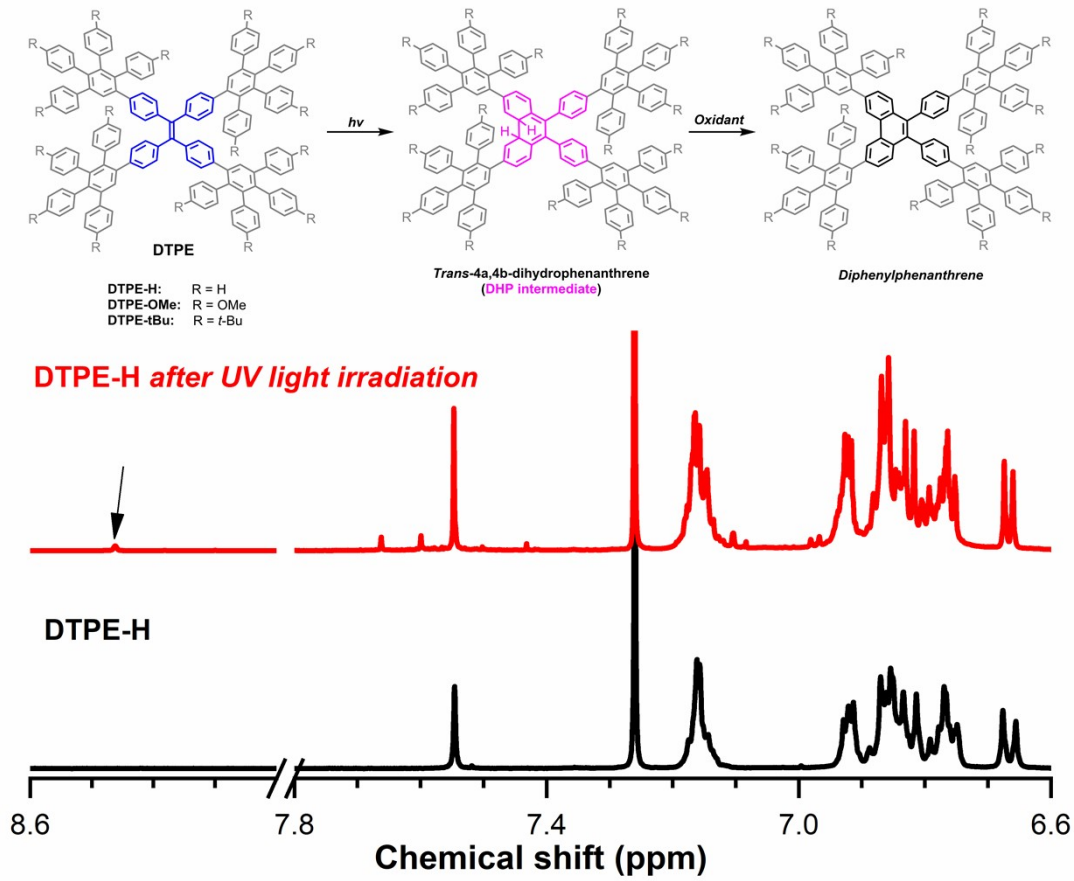

Figure S23. ^{1}H NMR of **DTPE-H** before and after photo-irradiation in $CDCl_3$ and proposed photocyclization reaction of **DTPEs**.

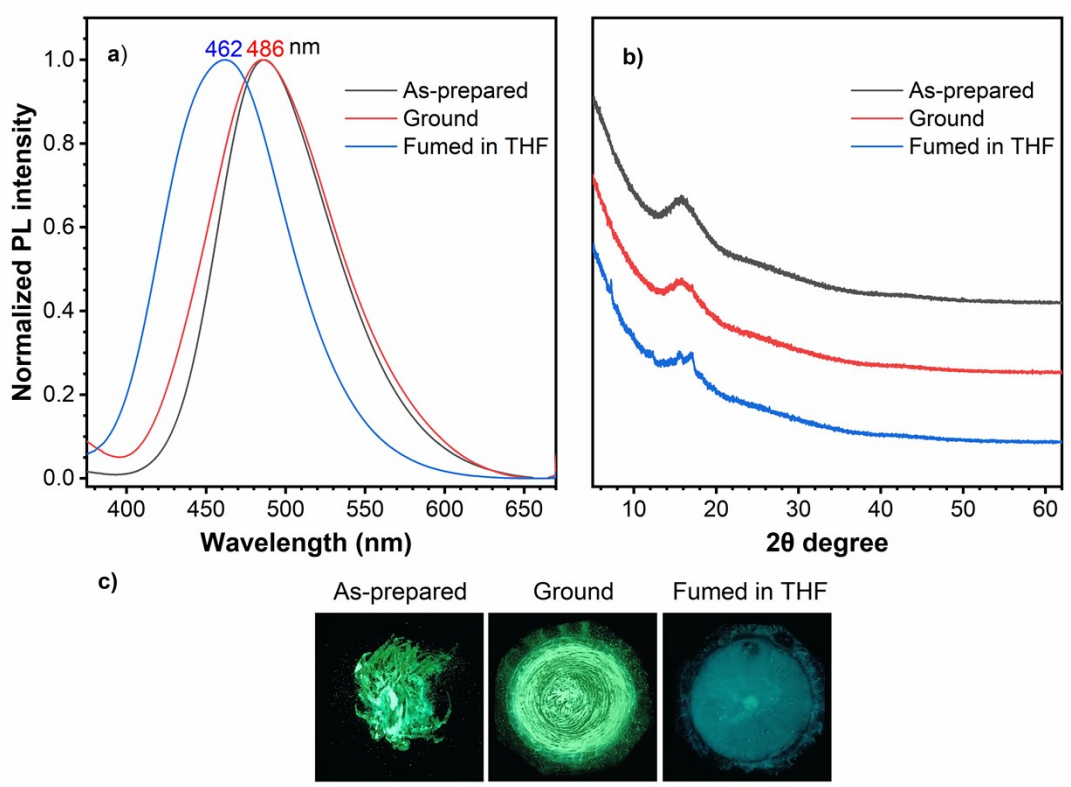

Figure S24. PL spectra (a), powder XRD results (b), and fluorescent images (c) of the as-prepared **DTPE-*t*Bu** samples after grinding and subsequent solvent fuming with THF vapours for 60 minutes.

4. NMR spectra

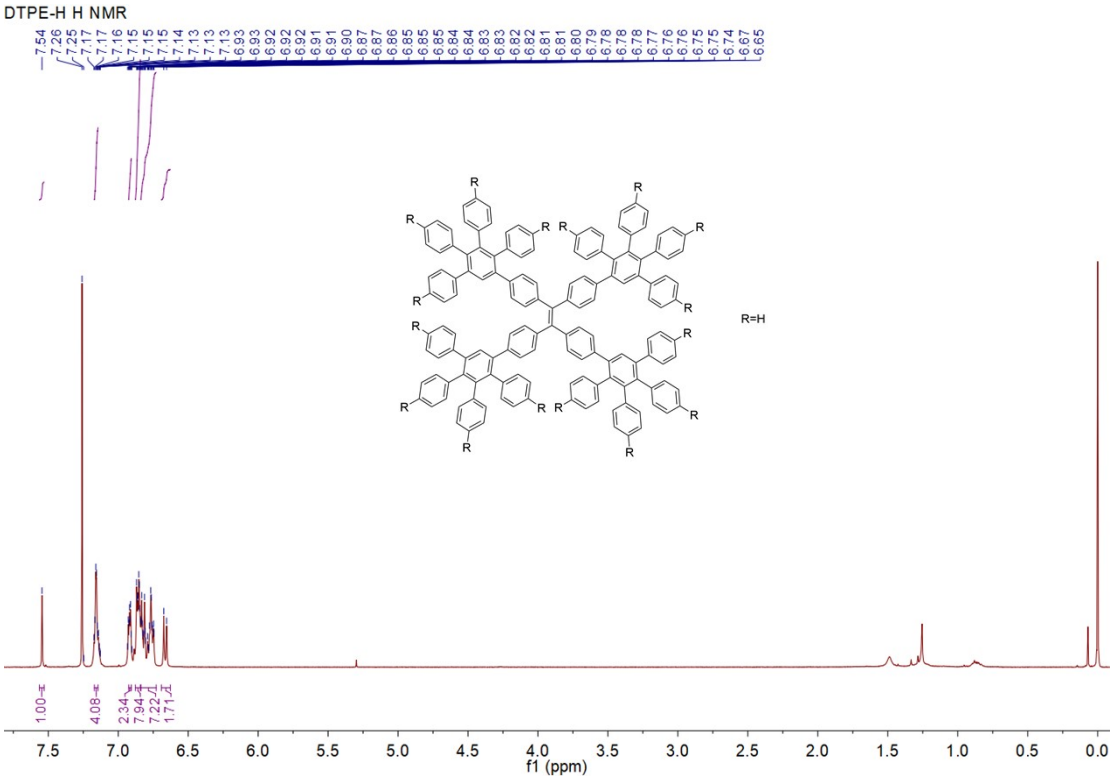

Figure S25. ^{1}H NMR spectrum of compound **DTPE-H** in $CDCl_3$ at 298K.

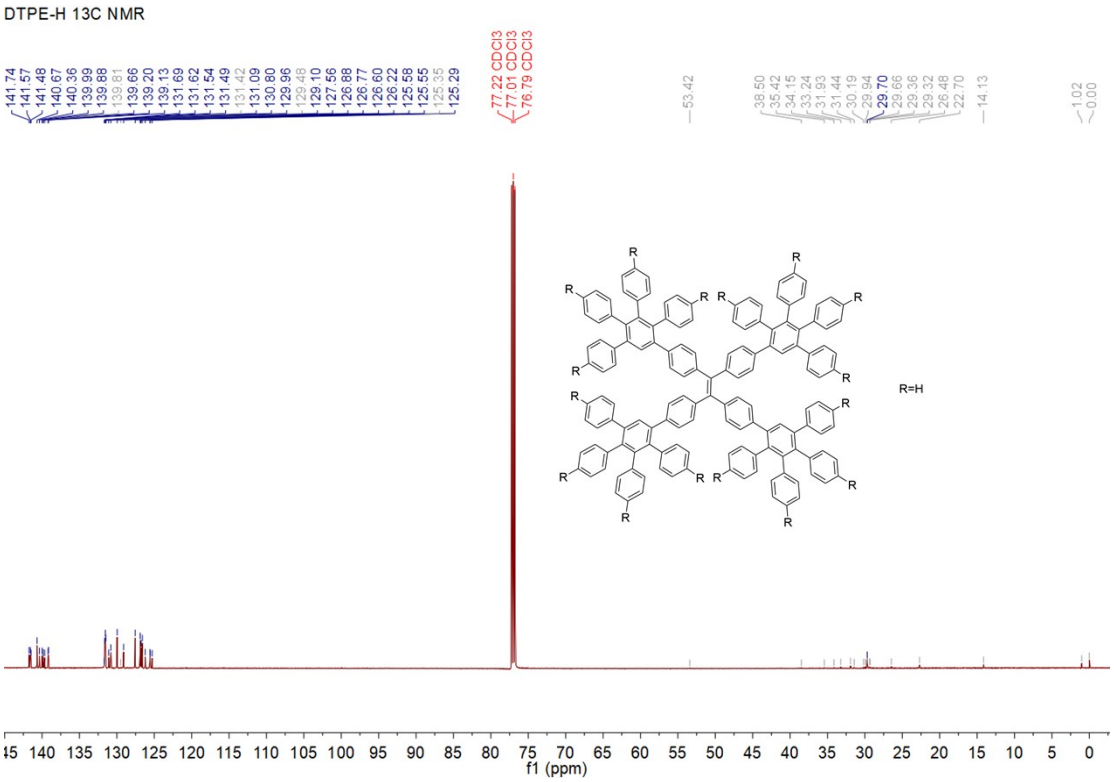

Figure S26. ^{13}C NMR spectrum of compound **DTPE-H** in $CDCl_3$ at 298K.

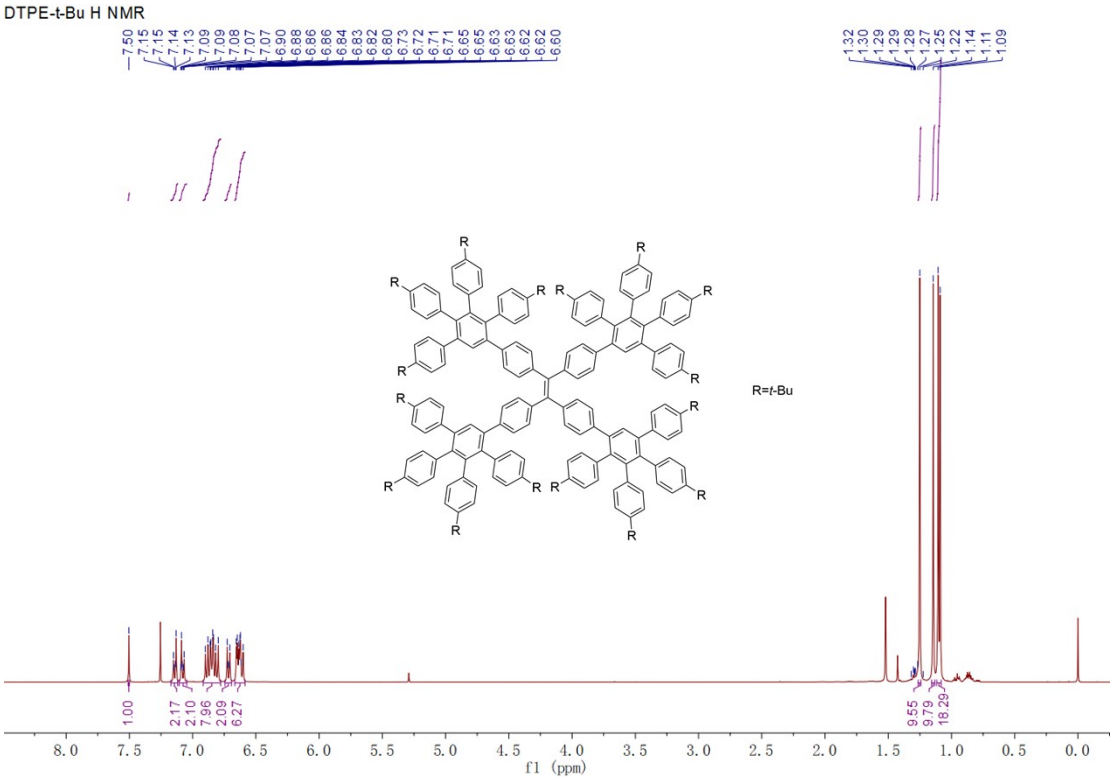

Figure S27. ^{1}H NMR spectrum of compound **DTPE-*t*Bu** in $CDCl_3$ at 298K.

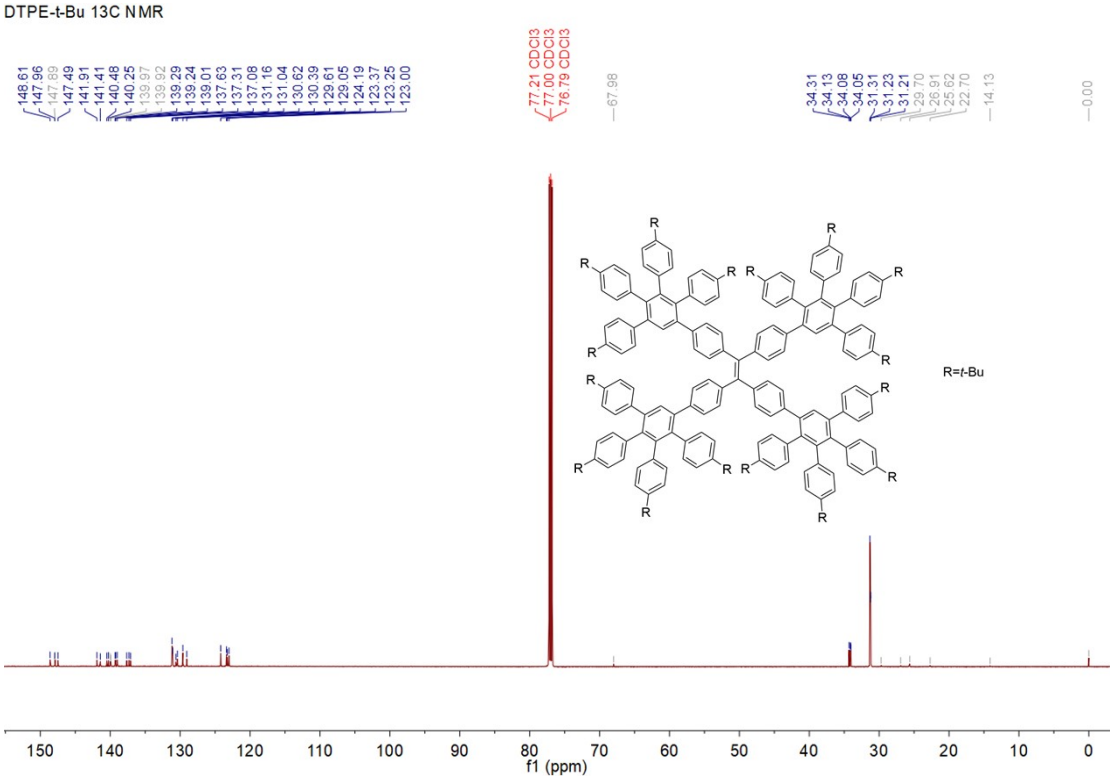

Figure S28. ^{13}C NMR spectrum of compound **DTPE-*t*Bu** in $CDCl_3$ at 298K.

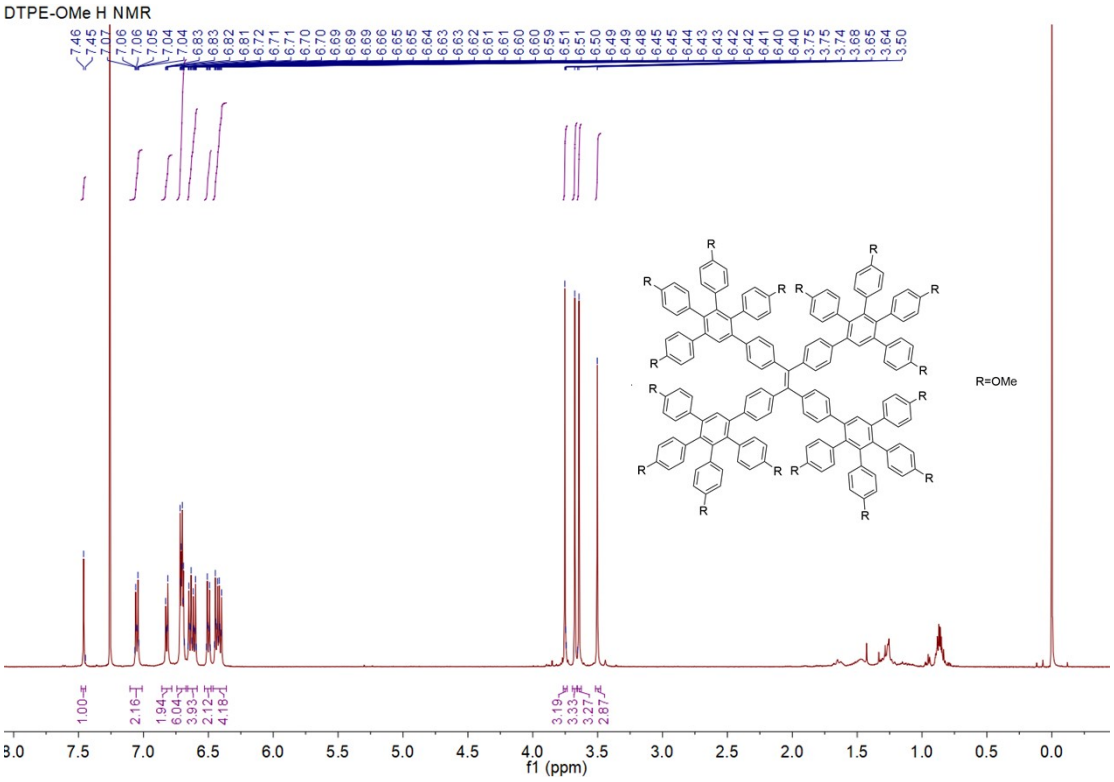

Figure S29. ^{1}H NMR spectrum of compound **DTPE-OMe** in $CDCl_3$ at 298K.

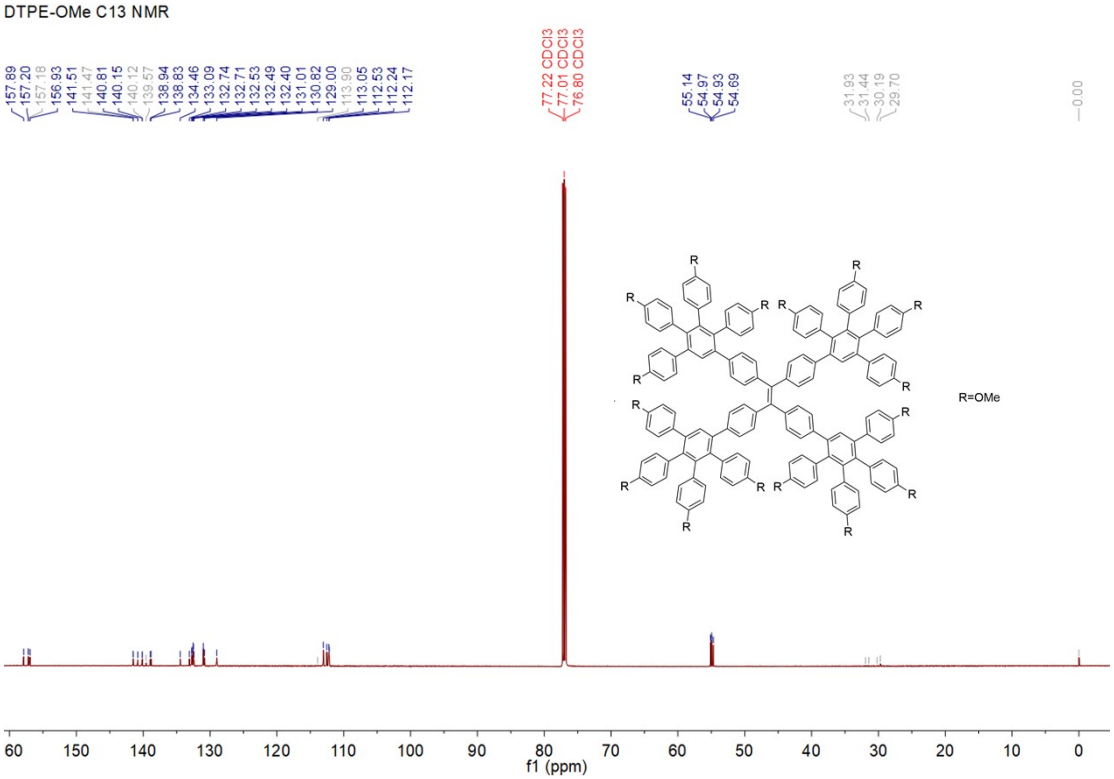

Figure S30. ^{13}C NMR spectrum of compound **DTPE-OMe** in $CDCl_3$ at 298K.

Reference:

(1) Xie, Y.; Tu, J.; Zhang, T.; Wang, J.; Xie, Z.; Chi, Z.; Peng, Q.; Li, Z. Mechanoluminescence from Pure Hydrocarbon Aiegen. *Chem. Commun.* **2017**, *53*, 11330-11333.

(2) Garg, V.; Kodis, G.; Liddell, P. A.; Terazono, Y.; Moore, T. A.; Moore, A. L.; Gust, D. Artificial Photosynthetic Reaction Center with a Coumarin-Based Antenna System. *The Journal of Physical Chemistry B* **2013**, *117*, 11299-11308.

(3) Gaussian 09, Revision D.01, M. J. Frisch, G. W. Trucks, H. B. Schlegel, G. E. Scuseria, M. A. Robb, J. R. Cheeseman, G. Scalmani, V. Barone, B. Mennucci, G. A. Petersson, H. Nakatsuji, M. Caricato, X. Li, H. P. Hratchian, A. F. Izmaylov, J. Bloino, G. Zheng, J. L. Sonnenberg, M. Hada, M. Ehara, K. Toyota, R. Fukuda, J. Hasegawa, M. Ishida, T. Nakajima, Y. Honda, O. Kitao, H. Nakai, T. Vreven, J. A. Montgomery, Jr., J. E. Peralta, F. Ogliaro, M. Bearpark, J. J. Heyd, E. Brothers, K. N. Kudin, V. N. Staroverov, T. Keith, R. Kobayashi, J. Normand, K. Raghavachari, A. Rendell, J. C. Burant, S. S. Iyengar, J. Tomasi, M. Cossi, N. Rega, J. M. Millam, M. Klene, J. E. Knox, J. B. Cross, V. Bakken, C. Adamo, J. Jaramillo, R. Gomperts, R. E. Stratmann, O. Yazyev, A. J. Austin, R. Cammi, C. Pomelli, J. W. Ochterski, R. L. Martin, K. Morokuma, V. G. Zakrzewski, G. A. Voth, P. Salvador, J. J. Dannenberg, S. Dapprich, A. D. Daniels,

O. Farkas, J. B. Foresman, J. V. Ortiz, J. Cioslowski, and D. J. Fox, Gaussian, Inc., Wallingford CT, 2013.

(4) Bo-Wen Wang, Kai Jiang, Dr. Jian-Xiao Li, Dr. Shi-He Luo, Prof. Dr. Zhao-Yang Wang, Prof. Dr. Huan-Feng Jiang. 1,1-Diphenylvinylsulfide as a Functional AIEgen Derived from the Aggregation-Caused-Quenching Molecule 1,1-Diphenylethene through Simple Thioetherification. *Angew. Chem. Int. Ed*. **2020**, *59*, 2338.

(5) Dr. Si-Hong Chen, Dr. Shi-He Luo, Dr. Long-Jiang Xing, Dr. Kai Jiang, Yan-Ping Huo, Qi Chen, Prof. Zhao-Yang Wang. Pentacenequinone derivatives: aggregation-induced emission enhancement, mechanism and fluorescent aggregates for superamplified detection of nitroaromatic explosives. *J. Mater. Chemistry C*. **2014**, *2*: 7356–7363.

(6) Pinrat O, Boonkitpatarakul K, Paisuwan W, Sukwattanasinitt M, Ajavakom A. Rational Design and Facile Synthesis of Dual-State Emission Fluorophores: Expanding Functionality for the Sensitive Detection of Nitroaromatic Compounds. *Chem. Eur. J.* **2022**, *28*, e202103478.

(7) Jason C. Sanchez, Antonio G. DiPasquale, Arnold L. Rheingold, and William C. Trogler. Synthesis,

Luminescence Properties, and Explosives Sensing with 1,1-Tetraphenylsilole- and 1,1-Silafluorene-vinylene Polymers. *Chemistry of Materials* **2007**, *19*, 6459-6470.

(8) Mengxia Gao, Yue Wu, Bin Chen, Bairong He, Han Nie, Tingyan Li, Fupeng Wu, Wenjun Zhou, Jian Zhou, Zujin Zhao. Di(naphthalen-2-yl)-1,2-diphenylethene-based conjugated polymers: aggregation-enhanced emission and explosive detection. *Polymer Chemistry*, **2015**, *6*, 7641-7645.

(9) Adil, Laxmi Raman. Gopikrishna. Peddaboodi. Krishnan Iyer. Parameswar. Receptor-Free Detection of Picric Acid: A New Structural Approach for Designing Aggregation-Induced Emission Probes. *ACS Applied Materials & Interfaces* **2018** *10* , 27260-27268.

(10) Yu, Jie. Tang, Chunlin. Gu, Xinggui. Zheng, Xiaoyan. Yu, Zhen-Qiang. He, Zikai. Li, Xin-Gui. Tang, Ben Zhong. Highly emissive phenylene-expanded [5]radialene. *Chem. Commun*., **2020**, *56*, 3911-3914.

(11) S.-H. Chen, S.-H. Luo, L.-J. Xing, K. Jiang, Y.-P. Huo, Q. Chen, Z.-Y. Wang. Rational Design and Facile Synthesis of Dual-State Emission Fluorophores: Expanding Functionality for the Sensitive Detection of Nitroaromatic Compounds. *Chem. Eur. J.* **2022**, *28*, e202103478.